Contents lists available at ScienceDirect

Digital Chinese Medicine

journal homepage: http://www.keaipublishing.com/dcmed

Mechanism of Wenyang Shengji Ointment in treating diabetic wounds based on network pharmacology and animal experiments

DING Yarong[a, b], XIE Chenlei[a], FENG Shuihua[b], YUAN Zhonghang[a], WANG Wei[a], LIU Mulin[a], ZHOU Zhongzhi[b*], CHEN Li[a*]

a. Hunan Provincial Key Laboratory of Vascular Biology and Translational Medicine, Hunan University of Chinese Medicine, Changsha, Hunan 410208, China

b. Department of Burns, Sores and Plastic Surgery, The First Hospital of Hunan University of Chinese Medicine, Changsha, Hunan 410007, China

ARTICLE INFO

Article history
Received 19 July 2023
Accepted 20 December 2023
Available online 25 March 2024

Keywords
Wenyang Shengji Ointment
Diabetic wound
Wound healing
Network pharmacology
Molecular docking
Hypoxia inducible factor 1A (HIF1A)

ABSTRACT

Objective To explore the mechanism of Wenyang Shengji Ointment (温阳生肌膏, WYSJO) in the treatment of diabetic wounds from the perspective of network pharmacology, and to verify it by animal experiments.

Methods The Traditional Chinese Medicine Systems Pharmacology Database and Analysis Platform (TCMSP) and related literature were used to screen active compounds in WYSJO and their corresponding targets. GeneCards, Online Mendelian Inheritance in Man (OMIM), DrugBank, PharmGkb, and Therapeutic Target Database (TTD) databases were employed to identify the targets associated with diabetic wounds. Cytoscape 3.9.0 was used to map the active ingredients in WYSJO, which was the diabetic wound target network. Search Tool for the Retrieval of Interaction Gene/Proteins (STRING) platform was utilized to construct protein-protein interaction (PPI) network. Kyoto Encyclopedia of Genes and Genomes (KEGG) and Gene Ontology (GO) enrichment analyses were performed to identify signaling pathways between WYSJO and diabetic wounds. AutoDock 1.5.6 was used for molecular docking of core components in WYSJO to their targets. Eighteen rats were randomly divided into control, model, and WYSJO groups (n = 6). The model and WYSJO groups were used to prepare the model of refractory wounds in diabetes rats. The wound healing was observed on day 0, 5, 9, and 14 after treatment, and the wound tissue morphology was observed by hematoxylin-eosin (HE) staining. The expression levels of core genes were detected by quantitative real-time polymerase chain reaction (qPCR).

Results A total of 76 active compounds in WYSJO, 206 WYSJO drug targets, 3 797 diabetic wound targets, and 167 diabetic wound associated WYSJO targets were screened out through network pharmacology. With the use of WYSJO-diabetic wound target network, core targets of seven active compounds encompassing quercetin, daidzein, kaempferol, rhamnetin, rhamnocitrin, strictosamide, and diisobutyl phthalate (DIBP) in WYSJO were found. GO enrichment analysis showed that the treatment of diabetes wounds with WYSJO may involve lipopolysaccharide, bacteria-derived molecules, metal ions, foreign stimuli, chemical stress, nutrient level, hypoxia, and oxidative stress in the biological processes. KEGG enrichment analysis showed that the treatment of diabetes wounds with WYSJO may involve advanced glycation end products (AGE-RAGE), p53, interleukin (IL)-17, tumor necrosis factor (TNF),

*Corresponding author: CHEN Li, E-mail: chenli_zyy@163.com. ZHOU Zhongzhi, E-mail: 3z_cl@163.com.

Peer review under the responsibility of Hunan University of Chinese Medicine.

DOI: 10.1016/j.dcmed.2024.04.009

Citation: DING YR, XIE CL, FENG SH, et al. Mechanism of Wenyang Shengji Ointment in treating diabetic wounds based on network pharmacology and animal experiments. Digital Chinese Medicine, 2024, 7(1): 79-89.

hypoxia inducible factor-1 (HIF-1), apoptosis, lipid, atherosclerosis, etc. The results of animal experiments showed that WYSJO could significantly accelerate the healing process of diabetic wounds ($P < 0.05$), alleviate inflammatory response, promote the growth of granulation tissues, and down-regulate the expression levels of eight core genes [histone crotonyltransferase p300 (*EP300*), protoc gene-oncogene c-Jun (*JUN*), myelocytomatosis (*MYC*), hypoxia inducible factor 1A (*HIF1A*), mitogen-activated protein kinase 14 (*MAPK14*), specificity protein 1 (*SP1*), tumor protein p53 (*TP53*), and estrogen receptor 1 (*ESR1*)] predicted by the network pharmacology ($P < 0.05$).

Conclusion The mechanism of WYSJO in treating diabetes wounds may be closely related to AGE-RAGE, p53, HIF-1, and other pathways. This study can provide new ideas for the pharmacological research of WYSJO, and provide a basis for its further transformation and application.

1 Introduction

In 1972, CATTERALL et al. [1] proposed that diabetic wounds were a prevalent form of chronic and refractory wounds on the body surface caused by peripheral neuropathy, infection, and tissue ischemia. Endogenous changes in nerves, blood vessels, immunity, and metabolism, as well as exogenous factors such as infections, traumas, and pressure collectively lead to the occurrence of refractory diabetic wounds. The interaction among various pathogenic factors constitutes a complex pathophysiological process in diabetic wounds [2]. At present, clinical treatments for the wounds primarily include blood glucose control, nourishing nerves, expanding blood vessels, vascular reconstruction and debridement, wound suction and sealing, and the regenerative medicine treatment. However, as many treatments as there are, a better treatment approach is still necessary due to the unpredictable effects and high cost of the existing treatments.

Traditional Chinese medicine (TCM) defines diabetic wounds as “stubborn sores” due to their lingering and refractory traits. Most of the diabetic wounds are “Yin syndrome” wounds. Therefore, ZHOU Zhongzhi, director of The First Hospital of Hunan University of Chinese Medicine, developed Wenyang Shengji Ointment (温阳生肌膏, WYSJO) including Dingxiang (Caryophylli Flos), Rougui (Cinnamoni Cassiae), Ruxiang (Resina Olibani), and Moyao (Myrrha) based on his clinical experience for many years. WYSJO has been playing a significant role in the treatment of diabetic ulcer since its employment in the clinics five years ago. Dingxiang (Caryophylli Flos), warm in nature and pungent in taste, can regulate the spleen and kidney meridians, warm the middle, reduce adverse reactions, tonify the kidney and assist Yang; Rougui (Cinnamoni Cassiae), with pungent taste and high heat nature, is able to tonify the kidney and spleen meridians by heating and unblocking meridians, dispelling cold and assisting Yang. When used together, their functions such as warming the kidney and spleen, dispelling cold, and assisting Yang, become stronger than being employed separately. Ruxiang (Resina Olibani) and Moyao (Myrrha) are warm in nature and pungent in taste, which target at the heart, liver, and spleen meridians to promote blood circulation and muscle growth. In previous clinical studies, WYSJO was applied externally on patients with chronic skin ulcers and pressure injuries, resulting in accelerated growth of wound granulation tissue, improved wound healing rate and reduced recurrence rate [3, 4]. It was suggested in some basic research that WYSJO significantly up-regulated the expression levels of CD34 and vascular endothelial growth factor (VEGF), promoted angiogenesis and accelerated wound healing process [5]. However, the mechanism of multi-targeted WYSJO for accelerating the healing process of diabetic wounds still remains unclear. Therefore, through the employment of network pharmacology and molecular docking methods, this paper screened main active ingredients in WYSJO and its potential targets for promoting the healing process of diabetic wounds, providing a theoretical basis for in-depth research on WYSJO and references for clarifying the mechanisms of WYSJO in treating diabetic wounds.

2 Materials and methods

2.1 Reagents and instruments

All the medicinal materials of WYSJO were purchased and identified by ZHANG Zhiguo of The First Hospital of Hunan University of Chinese Medicine. Hematoxylin-eosin (HE) staining kit was purchased from Servicebio (China), RNA extraction kit from Tiangen (China), reverse transcription kit, and quantitative real-time polymerase chain reaction (qPCR) kit from Novoprotein (China).

Paraffin slicing machine (Leica, RM2235), automatic tissue embedding machine (Leica, HistoCore Arcadia),

fully automatic digital slide scanning system (3Dhiestech, Pannoramic MIDI II), and fluorescent qPCR instrument (Roche, LightCycler 96) were the main laboratory equipments utilized in the study.

2.2 Experimental animals

A total of 18 specific pathogen free (SPF)-grade male Sprague-Dawley (SD) rats with weights ranging from 180 to 220 g were purchased from Hunan Slake Jingda Experimental Animal Co., Ltd., with a license number of SCXK (Xiang) 2019-0004. The qualification certificate number of the facility is SYXK (Xiang) 2019-0009. The rats were housed in an environment with temperatures ranging from 20 to 22 °C, relative humidity maintained between 40% and 60%, and a 12 h light-dark cycle. The study protocol was reviewed by the Experimental Animal Ethics Committee of Hunan University of Chinese Medicine. All experimental operations were conducted in accordance with ethical standards in the Experimental Animal Center (LL2021030301).

2.3 Network pharmacology analysis

2.3.1 Screening of active components in WYSJO Traditional Chinese Medicine Systems Pharmacology (TCMSP) (tcmspw.com/tcmsp.php) database was adopted to screen out active compounds in WYSJO [Dingxiang (Caryophylli Flos), Rougui (Cinnamoni Cassiae), Ruxiang (Resina Olibani), and Moyao (Myrrha)]. According to the characteristics of percutaneous absorption of external drugs, criteria for screening included a molecular weight (MW) < 3 000, an Aliphatic and Aromatic Log P (AlogP) of 1 – 5, drug-like (DL) properties value ⩾ 0.18 [6, 7]. As Rougui (Cinnamoni Cassiae) did not meet the criteria of DL ⩾ 0.18 for active compounds, the screening criteria were adjusted to MW < 3 000, AlogP of 1 – 5, and DL ⩾ 0.1.

2.3.2 Prediction of target genes of WYSJO Corresponding targets of drug ingredients [Dingxiang (Caryophylli Flos), Rougui (Cinnamoni Cassiae), Ruxiang (Resina Olibani), and Moyao (Myrrha)] were downloaded from the TCMSP database, and were paired with the screened active compounds using Perl software (V 5.32.1) to obtain proteins targeted by the active compounds. The targets of the screened active compounds were imported into the UniProt database (www.uniprot.org/) by specifying the species function as “human”. Subsequently, the identified protein targets were validated with their corresponding UniProt IDs, and the associated genetic names were retrieved.

2.3.3 Disease related target genes Using “diabetic ulcer” and “diabetic wound” as keywords, a search was performed across five disease gene databases, including Genecards (www.genecards.org/), Online Mendelian Inheritance in Man (OMIM) (omim.org/), PharmGkb (www.pharmgkb.org/), Drugbank (go.drugbank.com/), and Therapeutic Target Database (TTD) (db.idrblab.net/ttd/). After integrating the results and removing the duplicates, the target genes related to diabetic wounds were obtained. A Venn diagram depicting the overlap of disease-related genes was drawn using R language 4.1.3.

2.3.4 Drug-target-disease network construction The overlapping genes between WYSJO targets and diabetic wound targets were obtained and visualized using a Venn diagram in R language 4.1.3. The Cytoscape 3.9.0 software was used to screen the active compounds and action targets, carry out network visual analysis, and construct a drug-target-disease network.

2.3.5 Construction of a protein-protein interaction (PPI) network diagram and screening of core targets The WYSJO action targets obtained in section 2.3.3 were imported into Search Tool for the Retrieval of Interaction Gene/Proteins (STRING) platform (string db. org) to facilitate the healing of diabetic wounds. The species was set as “Homo sapiens”, interactions with confidence higher than 0.9 was selected, and a PPI network was constructed. The PPI network diagram was uploaded into the Cytoscape 3.9.0 software, and the network was analyzed using the CytoNCA plug-in. The core nodes of the network were evaluated based on parameter values such as degree centrality (DC), betweenness centrality (BC), closeness centrality (CC), eigenvector centrality (EC), local average connection centrality (LAC), and network centrality (NC). The core nodes were identified based on the criteria that their DC, BC, CC, EC, LAC, and NC all exceeded the median. Subsequently, the core nodes were organized into subnets. The network’s topology analysis diagram was then constructed by enhancing the visual representation of the core nodes with the use of Cytoscape 3.9.0.

2.3.6 Gene Ontology (GO) and Kyoto Encyclopedia of Genes and Genomes (KEGG) enrichment analyses In order to further explore the potential biological mechanisms of key targets in WYSJO’s promotion of diabetic wound repair, the R software “ClusterProfiler” and “org.Hs.eg.db” were employed for conducting GO and KEGG enrichment analyses on the targets obtained in section 2.3.5. $P < 0.05$ was considered statistically significant, and the data was visualized using bioinformatics (www.bioinformatics.com.cn).

2.4 Molecular docking

In order to verify the interaction relationship between key active components and key targets predicted by network pharmacology, molecular docking was conducted between them. In the regulatory network of drug-target-disease, key active compounds and their targets were identified based on degree analysis, selecting those with high

degree values as the top contributors. The chemical structure of the key active compounds was retrieved in MOL2 format from PubChem database (pubchem.ncbi.nlm.nih.gov/) , and its energy was minimized using ChemOffice software (V 21.0). The three dimension (3D) structure of the key target protein was retrieved from the ProteinData Bank (PDB) database (http://www.rcsb. org) and saved as PDB format. After removing water and ligand processing with the use of PyMOL software (V 2.5.8), molecular docking was carried out between the active compounds and their protein receptors using AutoDock 1.5.6. The results were saved as PDBQT format, and the docking outcomes were visualized using PyMOL software.

2.5 Animal experiment verification

2.5.1 Animal grouping and intervention approaches A total of 18 rats were randomized into control, model, and WYSJO groups (n = 6). Control group was injected with normal saline and wound preparation was performed simultaneously as the other two groups. The size and depth of the wounds were consistent across all groups, but no intervention was performed on control group after wound creation. Rats in model and WYSJO groups underwent wound modeling, after which, those in model group remained untreated, while those in WYSJO group underwent daily application of coin-sized WYSJO on the wound site starting from the 3rd day after modeling.

2.5.2 Establishment of skin defect model in diabetic rats The procedures were as follows: streptozotocin (STZ) was injected intraperitoneally at a dose of 50 mg/kg. Subsequently, hydrocortisone 20 mg/kg was injected intramuscularly for 7 d. Blood glucose levels were measured every 7 d, and the diabetic model was considered successful when the blood glucose value exceeded 16.7 mmol/L for one month. After successful modeling, intraperitoneal injection of 3% sodium pentobarbital was administered for anesthesia. Next, the dorsal skin was depilated, sterilized, and two prototype wounds with full-thickness skin defects were created with a perforator. After local observation, the successful establishment of the skin defect model in diabetic rats was achieved if the wound exhibited characteristics such as scattered appearance, flat collapse, slow growth of granulation, and a pale appearance [8].

2.5.3 Observation of the wound healing rate On day 0, 5, 9, and 14 after modeling, photographs were taken to record the wound healing process of rats in each group. A fixed measuring ruler was employed to cover the skin wounds of rats in each group during the recording process. The wound area of rats in each group was documented, and the wound healing rate was calculated using the formula: wound healing rate = (initial wound area – current wound area)/initial wound area × 100%.

2.5.4 HE staining The tissue was fixed with 4% paraformaldehyde, and a tissue block measuring 1 cm × 1 cm × 0.5 cm in size was prepared. The tissue block was then dehydrated, made transparent, wax immersed, embedded, sliced, and baked to prepare tissue sections. The slices were then placed in hematoxylin staining solution for 6 min, washed for 5 min, differentiated in 1% hydrochloric acid ethanol solution for 3 s, washed for 5 min, slowly rinsed in running tap water for 1 h, and dried naturally. Then they were stained in eosin dye for 5 min, rinsed with tap water for 5 min, and allowed to air dry. Next, the slices were dehydrated, placed in 95% ethanol for 5 min, then placed in 100% ethanol for 5 min, and allowed to dry. Dimethylbenzene was immersed twice for 5 min each time, and mounted with neutral resin. After the strips were air-dried for several days, the slices were swept using a digital sweep machine.

2.5.5 qPCR detection Total RNA was extracted using the Trizol method, which involved homogenization agents after chloroform layering, engaging in isopropyl alcohol precipitation, collecting the water layer, and purifying DNA by adding ethanol. The RNA was dissolved in diethyl pyrocarbonate (DEPC) water. Then, cDNA was synthesized by reverse transcription after measuring the concentration of RNA, which was later employed as template. The reaction system was configured according to a certain proportion, and was placed in a fluorescence qPCR instrument for amplification. Detailed primer sequences are listed in Table 1. The amplification was conducted under predenaturation at 95 °C for 60 s. A total of 45 cycles of denaturation were subsequently performed at 95 °C for 15 s, followed by annealing at 60 °C for 15 s. The relative mRNA expression levels of each factor were calculated using the $2^{-\Delta\Delta Ct}$ method. Due to the deviation of some data, the later data were kept as n = 4 for analysis in order to control the consistency of the number.

2.6 Statistical analysis

SPSS 26.0 software was used for data processing and analysis. If the data followed normal distribution and homogeneity of variance, it was expressed as mean ± standard deviation (SD). The t test was used for comparison between groups, and one-way analysis of variance (ANOVA) was used for among-group comparison. If normal distribution and homogeneity of variance were not satisfied, the Kruskal-Wallis H test was used. $P < 0.05$ was considered statistically significant.

3 Results

3.1 Active ingredients of WYSJO

According to the characteristics of percutaneous absorption of external drugs, a total of 77 active compounds were identified, including those found in Dingxiang

Table 1 List of primer sequences

Gene symbol	UniProt ID	Primer sequence (5' → 3')
EP300	Q09472	F: ACCTTCTCCTGTTCCTAGCCGTAC
		R: AATTGCTGTTGCTGCTGGTTGTTG
ESR1	P03372	F: TCCTCCTCATCCTTTCCCATATCCG
		R: GCATCTCCAGCAGCAGGTCATAG
HIF1A	Q16665	F: CCGCCACCACCACTGATGAATC
		R:GTGAGTACCACTGTATGCTGATGCC
JUN	P0541122	F: CTTCTACGACGATGCCCTCAACG
		R: AGGTTCAAGGTCATGCTCTGCTTC
MAPK14	P49137	F: GATAAGAGGATCACAGCAGCCCAAG
		R: TCGTAGGTCAGGCTCTTCCATTCG
MYC	P01106	F: AGCAGCGACTCTGAAGAAGAACAAG
		R: GGATGACCCTGACTCGGACCTC
SP1	P08047	F: GGCAGACTAGCAGCAGCAATACC
		R: ATGGAGGACAGTTGAGCAGCATTC
TP53	Q9ULZ0	F: CCTTACCATCATCACGCTGGAAGAC
		R: AGGACAGGCACAAACACGAACC

F, forward primer. R, reverse primer. *EP300*, histone crotonyltransferase p300. *ESR1*, estrogen receptor 1. *HIF1A*, hypoxia inducible factor 1A. *JUN*, protoc gene-oncogene c-Jun. *MAPK14*, mitogen-activated protein kinase 14. *MYC*, myelocytomatosis. *SP1*, specificity protein 1. *TP53*, tumor protein p53.

(Caryophylli Flos) (8), Rougui (Cinnamoni Cassiae) (11), Ruxiang (Resina Olibani) (8), and Moyao (Myrrha) (50). After eliminating duplicates, 76 active compounds remained.

3.2 Intersected targets between WYSJO and diabetic wounds

A total of 206 WYSJO targets were obtained through TCMSP database screening. With the assistance of Genecards, OMIM, drugbank, TTD, and PharmaGkb, a total of 3 797 diabetic wound targets were obtained. In the end, a total of 167 intersected targets between the two were identified (Figure 1).

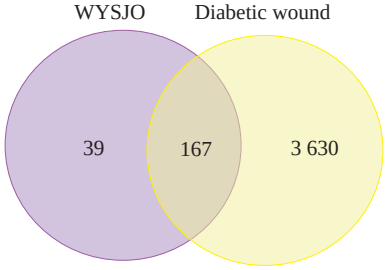

Figure 1 Intersected targets between WYSJO and diabetic wound

3.3 Construction of the regulatory network for WYSJO targets in diabetic wounds

As shown in Figure 2, the network comprised 243 nodes, including 76 active compounds and 167 potential target

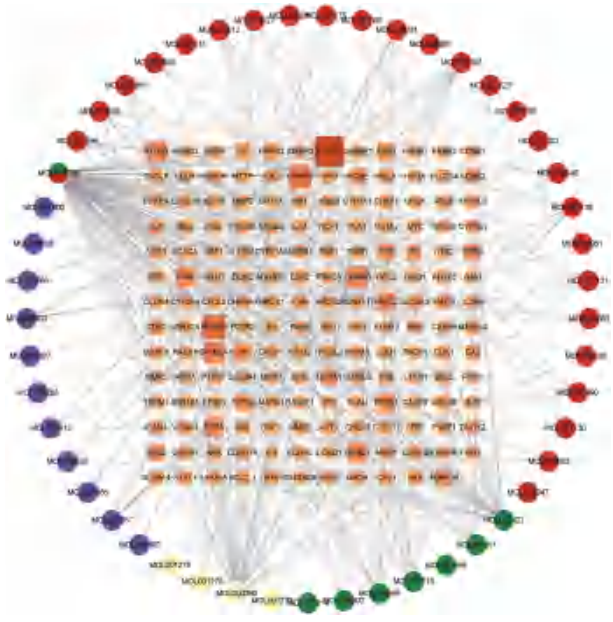

Figure 2 WYSJO-active compounds-target-diabetic wound regulatory network

The circular nodes represent the effective active compounds in WYSJO, the square nodes represent the potential target, and the lines represent the interaction among the three. The larger the node area in the figure is, the more important it is in the network. Size of the box and depth of color reflected the degree of correlation between the response and the active compounds. Red round node, active compounds of Moyao (Myrrha). Green round node, active compounds of Dingxiang (Caryophylli Flos). Blue round node, active compounds of Rougui (Cinnamoni Cassiae). Yellow round node, active compounds of Ruxiang (Resina Olibani). Two colors superimposed in the circle represented active compounds shared by two herbs.

nodes. Through screening, it was found that the connection density between seven components and the target was higher than the average overall density (Table 2).

Table 2 Components of the density attached to the targets

MOL number	Name	Degree	Betweenness value
MOL000098	Quercetin	117	28 469.725
MOL000390	Daidzein	47	9 310.282
MOL000422	Kaempferol	43	5 575.388
MOL005889	Rhamnetin	18	869.561
MOL000251	Rhamnocitrin	16	817.836
MOL013219	Strictosamide	16	811.205
MOL000057	DIBP	10	1 002.902

DIBP, diisobutyl phthalate.

3.4 Construction and analysis of the potential PPI network of WYSJO targets in treating diabetic wounds

The STRING database was employed to build a PPI network with the 167 intersected targets obtained above, resulting in 132 nodes and 441 lines (Figure 3A). The scoring value was acquired using CytoNCA analysis, and 41 network nodes were selected based on scores exceeding the median value, specifically, DC > 4, BC > 41.436, CC > 0.143, EC > 0.03, IC > 2.332, and LAC > 1.333 (Figure 3B). In the end, 15 network core nodes were filtered out, including HIF1A, Cyclin D1 (*CCND1*), mitogen-activated protein kinase 1 (*MAPK1*), *EP300*, *FOS*, *MAPK14*, *SP1*, *JUN*, cyclin-dependent kinase inhibitor 1A (*CDKN1A*), *TP53*, *AKT1*, *MYC*, *RB1*, *RELA*, and *ESR1* (Figure 3C).

3.5 GO and KEGG enrichment analyses

GO enrichment analysis revealed significant results with *P* value < 0.05, and the top 10 GO terms were selected to be depicted in the enrichment result circular graph (Figure 4A). Biological process (BP) primarily encompasses cell responses to various stimuli, including lipopolysaccharide, bacteria-derived molecules, metal ions, external stimuli, chemical stress, nutritional level, hypoxia, and oxidative stress. Cell component (CC) mainly involves various cell structures, including membrane raft, membrane microzone, organelle outer membrane, outer membrane, protein kinase complex, mitochondrial outer membrane, and endoplasmic reticulum cavity. Molecular function (MF) primarily involves activities, such as DNA binding transcription factor binding, RNA polymerase II specific DNA binding transcription factor binding, nuclear receptor activity, and ligand-activated transcription factor activity.

KEGG enrichment analysis revealed significant results with *P* value < 0.05, and the top 30 pathways were selected for data visualization analysis (Figure 4B). KEGG enrichment analysis shows that the treatment of diabetes wounds with WYSJO may involve advanced glycation end products-receptor for advanced glycation end products (AGE-RAGE), p53, IL-17, tumor necrosis factor (TNF), HIF-1 signaling pathways, apoptosis, lipid and atherosclerosis, and other related pathways.

3.6 Molecular docking

It is generally believed that when the binding energy of molecular docking is lower than 0 kcal/mol, molecules and ligands can effectively bind. When the binding energy is less than – 5 kcal/mol, it means that the molecules and ligands have good binding capacity. When the binding energy is less than or equal to – 7 kcal/mol, the molecules and ligands could bind tightly [9]. The top six pharmaceutical active compounds and the top eight gene targets screened by degree were used for molecular docking, and the results showed that quercetin could effectively bind to seven of the targets, and *EP300*, *HIF1A* and *JUN* were closely bound (Table 3). PyMOL was used to visually analyze the docking results of each core target that consumed the lowest binding energy (Figure 5).

3.7 Wound healing condition

The image of the wound on day 0, 5, 9, and 14 after modeling was documented, and the wound healing rates at each time point were calculated. After 5 d of intervention, except for model group, the wound tissue of the other

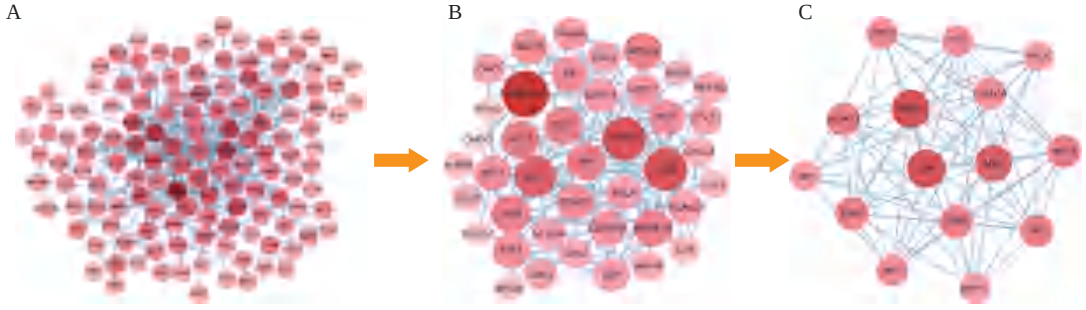

Figure 3 WYSJO active compounds target regulatory network

A, PPI network of common targets. B, PPI core network genes after the first screening. C, PPI core network genes after the second screening.

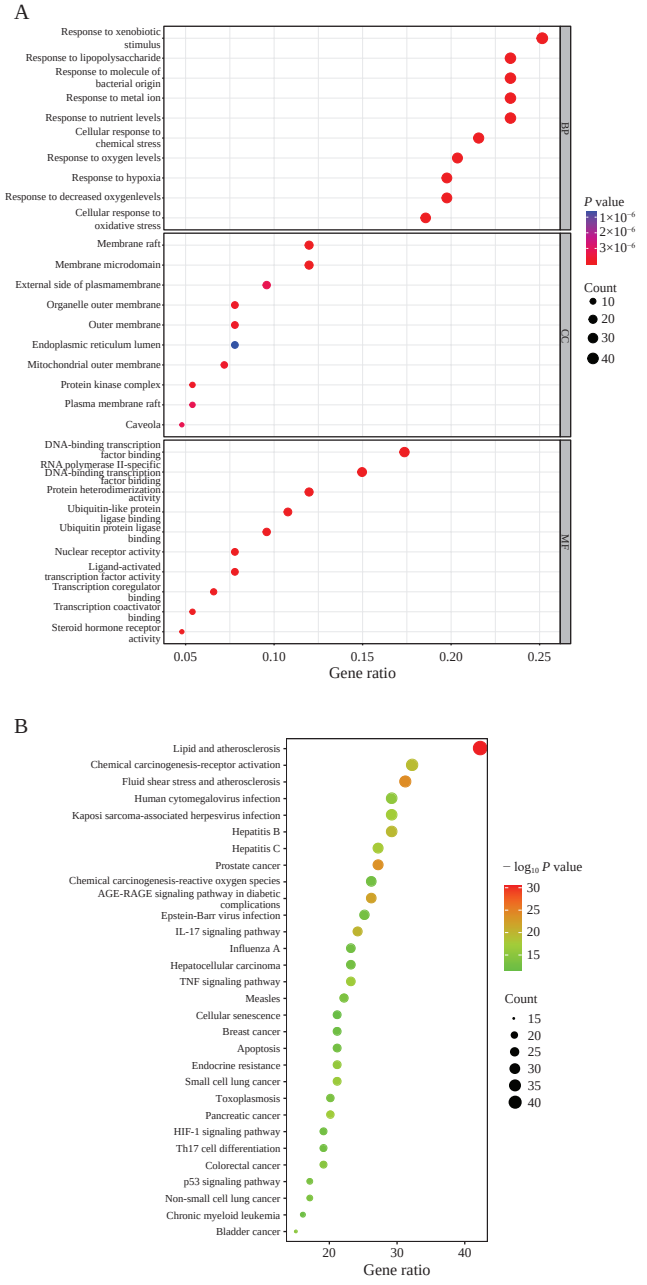

Figure 4 GO and KEGG enrichment analyses

A, the top 10 GO enrichment. B, the top 30 KEGG enrichment.

Table 3 Molecular docking results of quercetin and its key targets proteins

Component	Gene symbol	Binding energy (kcal/mol)
Quercetin	*EP300*	– 9.4
	HIF1A	– 8.0
	JUN	– 7.8
	MAPK14	– 4.9
	MYC	– 5.3
	TP53	– 3.9
	SP1	– 1.7

groups was dry and scabbed, the secretion basically disappeared, and the wound edge convergence was good. However, in model group, there were still more

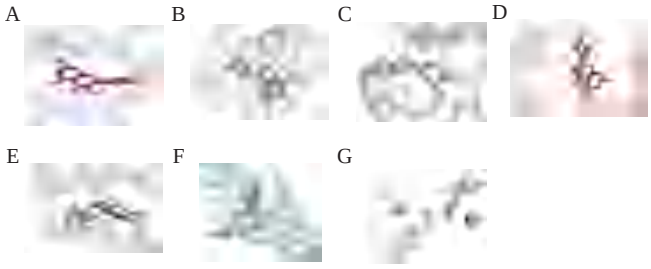

Figure 5 The molecular docking diagram of key components with target molecules

A, quercetin and *EP300*. B, quercetin and *HIF1A*. C, quercetin and *JUN*. D, quercetin and *MAPK14*. E, quercetin and *MYC*. F, quercetin and *TP53*. G, quercetin and *SP1*.

secretions, poor healing, and no obvious convergence of the wound margin. After 9 d of intervention, the wound edge and wound of model group were obviously red and swollen, and there were many red secretions, indicating that the wound did not heal obviously. However, the wounds of WYSJO group healed obviously, and the wound healing was good, with no obvious redness and swelling and other inflammatory manifestations. After 14 d of intervention, the wounds in control and WYSJO groups were basically healed. However, there was still a small amount of secretion and redness and swelling in the wounds of model group, with poor epithelization and poor wound condition (Figure 6A). After 5, 9, and 14 d of intervention, the wound healing rate of model group was

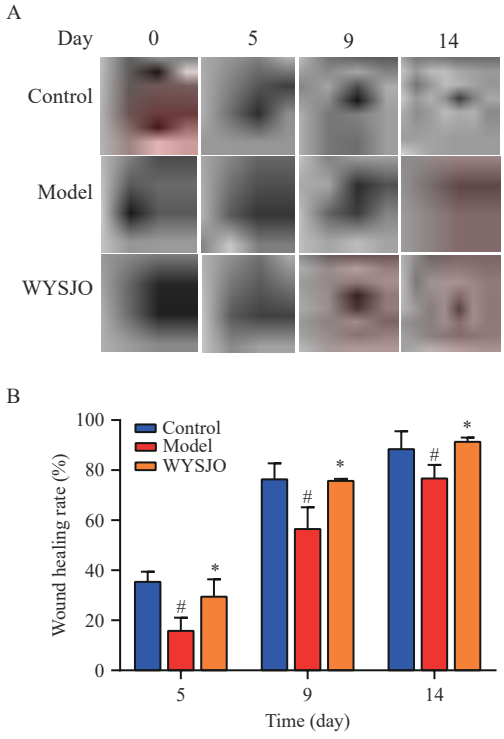

Figure 6 Wound healing condition

A, wound surface on day 0, 5, 9, and 14. B, wound healing rate on day 5, 9, and 14. Data were represented as mean ± SD (n = 4). $^{\#}P < 0.05$, compared with control group. $^{*}P < 0.05$, compared with model group.

significantly lower than control group ($P < 0.05$). Compared with model group, the wound healing rate of WYSJO group was significantly increased ($P < 0.05$) (Figure 6B).

3.8 Histomorphological changes

Following intervention for 14 d, the wound in control group exhibited substantial healing, characterized by reepithelialization. Fibroblasts were well-organized, collagen fibers formed an interwoven network. New skin appendages were also observed. In model group, only a small amount of scab had formed at the wound margin, and tissue edema and bleeding had not subsided. There were still erythrocyte extravasation and inflammatory cell infiltration, with cells demonstrating disorder, and the integrity of the skin structure was low. In WYSJO group, the wound had healed and scabbed. Inflammatory cells under the scab had subsided, the granulation tissue was mature, the new epidermis layer was thick and relatively complete, tissue cells were arranged in high order, thus indicating that the wound healed well (Figure 7).

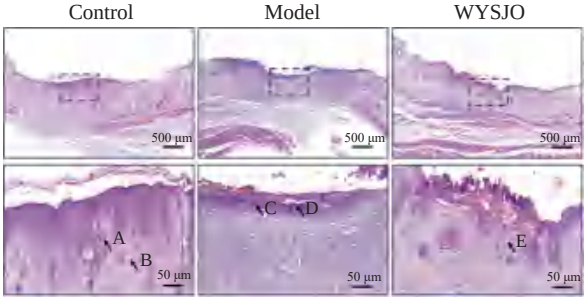

Figure 7 Observation of wound tissue morphology
A, skin appendages. B, collagen fibers. C, inflammatory cell infiltration. D, erythrocyte exudation. E, granulation tissue.

3.9 The expression levels of mRNA of key genes

When compared with control group, the mRNA expression levels of *EP300*, *JUN*, *MYC*, *HIF1A*, *MAPK14*, *SP1*, *TP53*, and *ESR1* genes in the wound skin tissue of rats in WYSJO group increased ($P < 0.05$); while in comparison with model group, the mRNA expression levels of *EP300*, *JUN*, *MYC*, *HIF1A*, *MAPK14*, *SP1*, *TP53*, and *ESR1* genes in the wound skin tissues of rats in WYSJO group decreased ($P < 0.05$) (Figure 8).

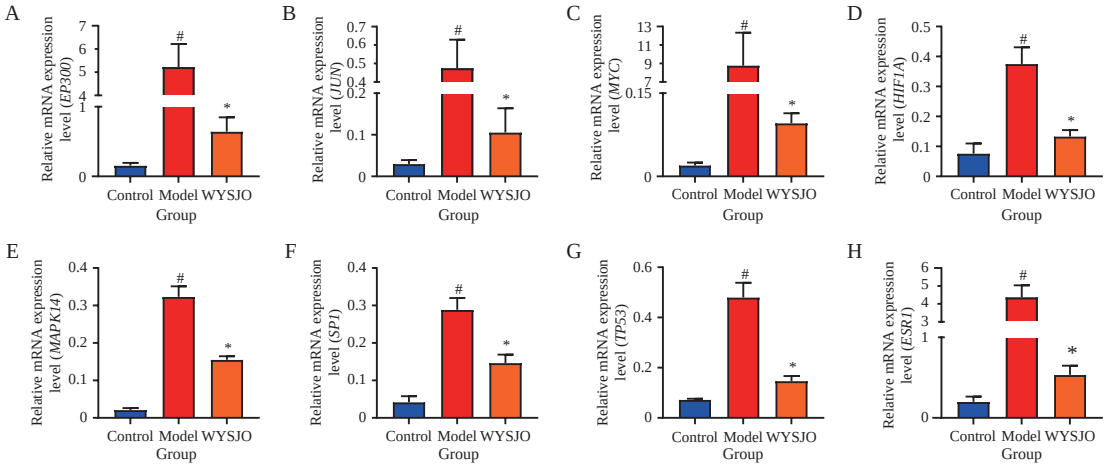

Figure 8 Effects of WYSJO on mRNA expression levels of key genes in wound skin tissues of rats
A, *EP300*. B, *JUN*. C, *MYC*. D, *HIF1A*. E, *MAPK14*. F, *SP1*. G, *TP53*. H, *ESR1*. Data were represented as mean ± SD ($n = 4$). $^{\#}P < 0.05$, compared with control group. $^{*}P < 0.05$, compared with model group.

4 Discussion

Diabetes, a significant chronic disease affecting the health of people in China, has a prevalence of 12.8% [10]. A series of pathological changes associated with diabetes renders the skin of affected individuals susceptible to damage, delayed healing, and recurrent ulceration, leading to the formation of challenge-to-heal wounds in diabetes patients. Due to the intricate pathogenesis of diabetic wounds, recent treatment methods have not succeeded in reversing the prolonged and challenging healing characteristics associated with this condition. Therefore, the treatment of diabetic wounds requires a comprehensive, multi-angle, and systematic treatment protocol, aligning with the integrated treatment TCM concept and its multifaceted targeting role. In this paper, WYSJO, which was effective in treating diabetic wounds, was analyzed for its drug composition, active ingredients, and target predictions to clarify its mechanism.

According to the Pharmacopoeia of the People's Republic of China 2020 [11], the content of the four herbs that make up WYSJO is determined by volatile oil or volatile oil components. Hence, volatile oil is the key component in WYSJO. In this network pharmacology analysis, it was found that among the top seven active ingredients, DIBP

and kaempferol belong to the volatile oils with good transdermal properties. Among them, kaempferol has been confirmed to significantly promote diabetic wound healing [12], and inhibit the activation of AGE-RAGE pathway by reducing AGEs, thereby inhibiting a series of subsequent oxidative stress damage and inflammatory stimulation [13]. Another major active ingredient, quercetin, has also been found to reduce the content of AGEs in the body, improve the balance between pro-oxidants and anti-oxidants, and prevent excessive oxidative stress damage [14]. This is consistent with our finding that the active components of WYSJO can affect wound healing by regulating the AGE-RAGE pathway. In addition, quercetin was found to have certain targeting effects with HIF1A and EP300 in this result. HIF-1 is a heterodimer composed of two subunits, A and B. Among them, HIF1A is the main transcriptional regulator for cells to adapt to hypoxia [15]. *EP300* is a lysine acetyltransferase that can initiate *HIF1A*-induced downstream transcription by binding to hypoxia response element (HRE) [16, 17]. However, there are different opinions about the protein encoded by *HIF1A* gene in diabetic wounds. Some believe that the expression level of *HIF1A* is increased due to the hypoxic environment of diabetes [18], and some believe that the expression level of *HIF1A* is significantly reduced by the influence of high glucose [19]. However, we found that *HIF1A* gene was highly expressed in diabetic wounds, and WYSJO reversed the high expression level of *HIF1A* and inhibited the expression level of *EP300*. However, a large number of literatures have found that wound healing can be promoted by promoting HIF/VEGF pathway [20]. Because there are many processes between genes and proteins, there may be different situations between the two. Moreover, the protein level was not detected in this experiment, so we cannot determine the expression level of *HIF1A* protein in diabetic wounds and after WYSJO intervention, and further research is needed.

This study found that WYSJO could reduce the inflammatory response of wound tissue, and the key regulatory pathways found in the prediction results were IL-17 and TNF signaling pathways, which were classic inflammation-related signaling pathways. ZHANG et al. [21] found that inhibition of IL-17 could inhibit the expressions of IL-1β and IL-6 and promote the expressions of angiogenesis related factors such as CD31 and PDGF, thus accelerating wound healing. In addition, HUANG et al. [22] found that TNF signaling pathway is heavily activated by the high glucose environment of diabetic wounds, releasing a large amount of IL-1β and IL-6, which makes macrophages polarized to M1 type, and the wound remains in the inflammatory stage for a long time, which is difficult to heal. In addition, TNF and IL-17 signaling activated *JUN* and *MAPK14* genes. The proteins encoded by *JUN* and *MAPK14* genes play important roles in promoting cell proliferation, regulating inflammation, and apoptosis. GRIFFIN et al. [23] found that *JUN* over expression could significantly increase VEGF, thereby promoting angiogenesis in wound tissue. WU et al. [24] can promote the proliferation of vascular endothelial cells and inhibit the activation of pro-inflammatory genes by knocking out *MAPK14*. We also demonstrated that *JUN* and *MAPK14* genes were significantly increased in diabetic wounds and their expression was significantly decreased by WYSJO intervention. Therefore, we speculated that WYSJO may inhibit the expression of *JUN* and *MAPK14* by inhibiting the TNF and IL-17 signaling pathways, and finally inhibit the inflammatory response to accelerate angiogenesis and promote wound healing. However, this experiment has only completed the prediction and gene level verification, and the above speculation needs to be further studied (Figure 9).

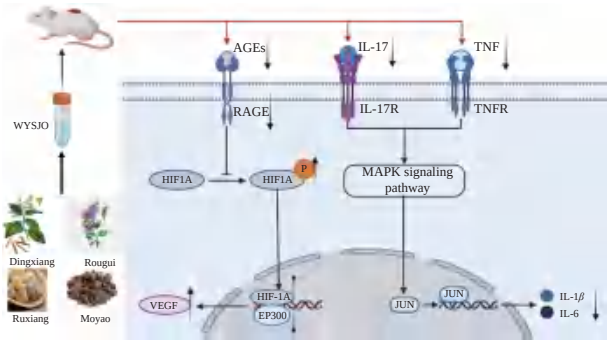

Figure 9 Mechanism of WYSJO in promoting diabetic wounds healing
P, phosphorylation.

5 Conclusion

This study carried out animal experiments and network pharmacology analysis for the investigation of the mechanisms of WYSJO, and identified the possible role of *EP300*, *JUN*, *MYC*, *HIF1A*, *MAPK14*, *SP1*, *TP53*, and *ESR1* in WYSJO, which serves as multiple targets. WYSJO might regulate hypoxia, oxidative stress and other reactions through AGE-RAGE, p53, IL-17, HIF1A, and other signaling pathways to promote diabetic wound healing, providing references for further research on WYSJO.

Fundings

National Natural Science Foundation of China (82074447), Key Research and development Project of Hainan Province (ZDYF2023SHFZ123), and Research Project of Traditional Chinese Medicine in Hunan Province (C2023038).

Competing interests

The authors declare no conflict of interest.

References

[1] CATTERALL WA, PEDERSEN PL. Adenosine triphosphatase from rat liver mitochondria. II. Interaction with adenosine diphosphate. The Journal of Biological Chemistry, 1972, 247(24): 7969–7976.

[2] ZHANG DY, YANG YL, HUANG H, et al. Research progress on pathological mechanism and treatment of diabetic foot. Journal of Shenyang Pharmaceutical University, 2021, 38(6): 636–642.

[3] WANG TT, CHEN L, LAN HW, et al. Clinical observation on 50 cases of chronic skin ulcer treated by Wenyang Shengji Gao. Journal of Gansu University of Chinese Medicine, 2021, 38(2): 46–50.

[4] XUN Y, ZHOU Y, YI X, et al. Clinical observation of Wenyang Shengji Gao combined with pedicled composite tissue flap in the treatment of pressure injury. China Modern Doctor, 2022, 60(12): 144–147.

[5] ZHANG HH, TANG JQ, ZHOU ZZ, et al. Effect of Wenyang Shengji Gao on the expressions of CD34 and VEGF in chronic wound and vascular reconstruction of diabetic rats with Yin Syndrome. Infection Inflammation Repair, 2021, 22(2): 67–71.

[6] ABDALLAH MH, ABU LILA AS, UNISSA R, et al. Preparation, characterization and evaluation of anti-inflammatory and anti-nociceptive effects of brucine-loaded nanoemulgel. Colloids and Surfaces B, Biointerfaces, 2021, 205: 111868.

[7] WANG Z, XIE XH, WANG MC, et al. Analysis of common and characteristic actions of *Panax ginseng* and *Panax notoginseng* in wound healing based on network pharmacology and meta-analysis. Journal of Ginseng Research, 2023, 47(4): 493–505.

[8] ZHOU JY, CHEN L, KANG HY, et al. Establishment of wound model of diabetes rats with Yin syndrome. Information on Traditional Chinese Medicine, 2023, 40(9): 46-53.

[9] PINZI LC, RASTELLI G. Molecular docking: shifting paradigms in drug discovery. International Journal of Molecular Sciences, 2019, 20(18): 4331.

[10] LI YZ, TENG D, SHI XG, et al. Prevalence of diabetes recorded in mainland China using 2018 diagnostic criteria from the American diabetes association: national cross sectional study. BMJ, 2020, 369: m997.

[11] Chinese Pharmacopoeia Commission. Pharmacopoeia of People's Republic of China: 2020 edition. Part I. Beijing: China Medical Science Press, 2020.

[12] ÖZAY Y, GÜZEL S, YUMRUTAŞ Ö, et al. Wound healing effect of kaempferol in diabetic and nondiabetic rats. The Journal of Surgical Research, 2019, 233: 284–296.

[13] KISHORE L, KAUR N, SINGH R. Effect of Kaempferol isolated from seeds of Eruca sativa on changes of pain sensitivity in Streptozotocin-induced diabetic neuropathy. Inflammopharmacology, 2018, 26(4): 993–1003.

[14] ZHAO YT, TANG Y, SANG SM. Dietary quercetin reduces plasma and tissue methylglyoxal and advanced glycation end products in healthy mice treated with methylglyoxal. The Journal of Nutrition, 2021, 151(9): 2601–2609.

[15] BOHUSLAVOVA R, CERYCHOVA R, PAPOUSEK F, et al. HIF-1α is required for development of the sympathetic nervous system. Proceedings of the National Academy of Sciences of the United States of America, 2019, 116(27): 13414–13423.

[16] XU DZ, LI C. Regulation of the SIAH2-HIF-1 axis by protein kinases and its implication in cancer therapy. Frontiers in Cell and Developmental Biology, 2021, 9: 646687.

[17] LI MY, MI CL, WANG KS, et al. Shikonin suppresses proliferation and induces cell cycle arrest through the inhibition of hypoxia-inducible factor-1α signaling. Chemico-Biological Interactions, 2017, 274: 58–67.

[18] ILEGEMS E, BRYZGALOVA G, CORREIA J, et al. HIF-1α inhibitor PX-478 preserves pancreatic β cell function in diabetes. Science Translational Medicine, 2022, 14(638): eaba9112.

[19] WAN J, BAO Y, HOU LJ, et al. lncRNA ANRIL accelerates wound healing in diabetic foot ulcers via modulating HIF1A/VEGFA signaling through interacting with FUS. The Journal of Gene Medicine, 2023, 25(2): e3462.

[20] WANG L, WU HW, XIONG L, et al. Quercetin downregulates cyclooxygenase-2 expression and HIF-1α/VEGF signaling-related angiogenesis in a mouse model of abdominal aortic aneurysm. BioMed Research International, 2020, 2020: 9485398.

[21] ZHANG JJ, ZHOU R, DENG LJ, et al. Huangbai liniment and berberine promoted wound healing in high-fat diet/streptozotocin-induced diabetic rats. Biomedecine & Pharmacotherapie, 2022, 150: 112948.

[22] HUANG SM, WU CS, CHIU MH, et al. High glucose environment induces M1 macrophage polarization that impairs keratinocyte migration via TNF-α: an important mechanism to delay the diabetic wound healing. Journal of Dermatological Science, 2019, 96(3): 159–167.

[23] GRIFFIN MF, BORRELLI MR, GARCIA JT, et al. JUN promotes hypertrophic skin scarring via CD36 in preclinical *in vitro* and *in vivo* models. Science Translational Medicine, 2021, 13(609): eabb3312.

[24] WU W, ZHANG W, CHOI M, et al. Vascular smooth muscle-MAPK14 is required for neointimal hyperplasia by suppressing VSMC differentiation and inducing proliferation and inflammation. Redox Biology, 2019, 22: 101137.

基于网络药理学联合动物实验探究温阳生肌膏治疗糖尿病创面的作用机制

丁雅容[a, b], 谢晨磊[a], 奉水华[b], 袁忠行[a], 王巍[a], 刘沐琳[a], 周忠志[b*], 陈丽[a*]

a. 湖南中医药大学血管生物学与转化医学湖南重点实验室, 湖南 长沙 410208, 中国
b. 湖南中医药大学第一附属医院烧伤疮疡整形科, 湖南 长沙 410007, 中国

【摘要】目的 从网络药理学角度探讨温阳生肌膏治疗糖尿病创面的作用机制，并通过动物实验进行验证。**方法** 采用中药系统药理学数据库与分析平台（TCMSP）及相关文献筛选温阳生肌膏（WYSJO）活性成分及对应靶点；通过 GeneCards、Online Mendelian Inheritance in Man（OMIM）、DrugBank、PharmGkb 和 Therapeutic Target（TTD）等数据库检索糖尿病创面的作用靶点；使用 Cytoscape 3.9.0 绘制出 WYSJO 活性成分-糖尿病创面靶标网络；应用检索相互作用基因/蛋白质的搜索工具（STRING）平台搭建蛋白互作网络（PPI）；应用京都基因与基因组百科全书（KEGG）与基因本体（GO）富集分析 WYSJO 与糖尿病创面的信号通路；应用 AutoDock 1.5.6 对核心成分与靶点进行分子对接；将 18 只大鼠随机分为对照组、模型组和 WYSJO 组（$n = 6$），以模型组和 WYSJO 组制备糖尿病大鼠难治性创面模型。分别在处理第 0、5、9、14 天时观察创面愈合，苏木素-伊红（HE）染色观察创面组织形态，实时荧光定量聚合酶链式反应（qPCR）检测核心基因表达情况。**结果** 网络药理学筛选出 WYSJO 药物有效成分 76 种，药物靶点 206 个，糖尿病创面疾病靶点 3 797 个，以及 WYSJO 治疗糖尿病创面作用靶点 167 个；通过构建 WYSJO 活性成分-糖尿病创面作用靶标网络，发现槲皮素、大豆苷元、山柰酚、鼠李素、鼠李柠檬素、异长春花苷内酰胺和邻苯二甲酸二异丁酯（DIBP）7 个核心靶点。GO 富集分析表明温阳生肌膏治疗糖尿病创面可能涉及细胞对脂多糖、细菌来源分子、金属离子、外来刺激、化学应激、营养水平、缺氧及氧化应激等生物过程。KEGG 富集分析表明温阳生肌膏治疗糖尿病创面可能涉及高级糖基化终末产物-受体（AGE-RAGE）信号通路、p53 信号通路、白介（IL）-17 信号通路、肿瘤坏死因子（TNF）信号通路、缺氧诱导因子-1（HIF-1）信号通路、细胞凋亡、脂质和动脉粥样硬化等相关通路发挥治疗糖尿病创面的作用。动物实验显示 WYSJO 可显著加快糖尿病创面的愈合速度（$P < 0.05$），减轻炎症反应，促进肉芽组织生长，同时也可下调网络药理学预测的 E1A 结合蛋白 p300（*EP300*）、Jun 激酶（*JUN*）、骨髓细胞瘤癌基因（*MYC*）、缺氧诱导因子 1A（*HIF1A*）、丝裂原活化蛋白激酶 14（*MAPK14*）、特异性蛋白 1（*SP1*）、肿瘤蛋白 p53（*TP53*）以及雌激素受体 1（*ESR1*）等 8 个核心基因表达（$P < 0.05$）。**结论** WYSJO 治疗糖尿病创面的作用机制可能与 AGE-RAGE、p53、HIF-1 等通路密切相关，通过此研究可为 WYSJO 的药理学研究提供新思路，并为其进一步转化应用提供基础。

【关键词】温阳生肌膏；糖尿病创面；创面愈合；网络药理学；分子对接；缺氧诱导因子 1A